ORIGINAL PAPER

RJME Romanian Journal of Morphology & Embryology http://www.rjme.ro/

# Remodeling of intramyocardial tissue capillaries density depending on age, sex and cause of death

LAURA ELENA CAMENIŢĂ[1)], RĂZVAN MIHAIL PLEŞEA[2)], CRISTINA FLORESCU[1,3)], MIRCEA-SEBASTIAN ŞERBĂNESCU[4)], IANCU EMIL PLEŞEA[5,6)], VALENTIN TITUS GRIGOREAN[5,7,8)], TIBERIU TĂTARU[9)]

[1)]*Doctoral School, University of Medicine and Pharmacy of Craiova, Romania*

[2)]*Department of Cell and Molecular Biology, University of Medicine and Pharmacy of Craiova, Romania*

[3)]*Department of Cardiology, University of Medicine and Pharmacy of Craiova, Romania*

[4)]*Department of Medical Informatics and Biostatistics, University of Medicine and Pharmacy of Craiova, Romania*

[5)]*Doctoral School, Carol Davila University of Medicine and Pharmacy, Bucharest, Romania*

[6)]*Department of Pathology, Bagdasar–Arseni Emergency Clinical Hospital, Bucharest, Romania*

[7)]*Department of Surgery, Carol Davila University of Medicine and Pharmacy, Bucharest, Romania*

[8)]*Department of General Surgery, Bagdasar–Arseni Emergency Clinical Hospital, Bucharest, Romania*

[9)]*Department of Health and Motricity, Constantin Brâncuşi University, Târgu Jiu, Romania*

## Abstract

*Aim*: Aging together with the wide range of diseases causing death are ones of the influential factors of cardiac wall remodeling regarding both their structural and functional features. The authors compared the changes of myocardial interstitial capillary network density (vascular density – VD) between the main regions of the cardiac wall during patients' ageing and depending on patients' cause of death. *Patients, Materials and Methods*: Five cross-sections from epicardium to endocardium [left ventricle wall (LVW): anterior segment (LV_AW), lateral segment (LV_LW), and posterior segment (LV_PW); interventricular septum (IVS); and right ventricle wall (RVW)] were collected during necropsies from 95 patients died with different ages (AP_01, 0–24 years; AP_02, 25–44 years; AP_03, 45–64 years; and AP_04, >64 years) and with different types of causes of death (V_P – vascular diseases, NV_P – non-vascular diseases, and S/V_Dth – suspect/violent cause of death, considered also control group – CG) in the hospital. Tissue samples were processed classically and immunomarked with anti-cluster of differentiation 34 (CD34) antibody. Glass slides were transformed into virtual slides. The VD was determined with a dedicated built program. Mean values (AVs) were compared with Pearson's correlation test. *Results*: On one hand, VD increased slowly from youth to elderly in LV_Ws and decreased with age in the IVS and RVW. It had the lowest values in LV_Ws till AP_03 and in RVW in elderly. The highest values were in RVW till 44 years and then in IVS. VD had higher values in women than in men along the main regions of the cardiac wall and a divergent behavior, with age, in the two sexes. Thus, in men, VD had an increasing trend with age from LV_AW to RVW [correlation matrix (CM) positive, *p*-value >0.05] whereas in women, the trend was decreasing with age from LV_AW to RVW (CM negative, *p*-value >0.05), excepting IVS where it increases (CM positive). On the other hand, the VD had lowest values in V_P group and highest values in CG in general and in both sexes. Its values increased from LVW to RVW in V_P group and CG and decreased in NV_P group in general and in both sexes. They also increased from LV_AW toward LV_PW in all groups of COD and in both sexes. The VD AVs were higher in females than in males in CG and NV_P group and higher in males than in females in V_P group. Its values were lowest in both sexes in V_P group but highest in men in NV_P group and in women in CG. *Conclusions*: VD and is remodeling with aging in different ways both along the cardiac wall's regions and in the two sexes, being generally higher in females than in males. The causing death diseases determine different pathways of interstitial capillary network remodeling both along the different regions of the cardiac wall and in the two sexes, the most important being the capillary density decrease in vascular diseases as compared with all other causes of death.

***Keywords***: myocardial vascular network, morphometry, age, sex, cause of death.

## Introduction

The myocardial tissue is subject to a continuous remodeling process regarding both of its structural and functional components, process influenced by two major categories of factors. One of them consists of the wide range of diseases and their subsequent lesions and the other is the biological event of aging whose most recognized influencers are caloric restriction, cell senescence, and free radicals. Both factors cause time-dependent and progressive accumulation of cellular morphological alterations, followed by functional alterations that result in loss of physiological integrity and increased vulnerability to death [1–7].

One of the main components of the myocardial tissue is the intramyocardial vascular network. It originates in the coronary arteries and consists of capillaries composed of only a single endothelial cells layer, with numerous bifurcations and anastomoses, forming a rich and dense meshwork embedded in the delicate sheath of endomysial connective tissue that surrounds myocardiocytes [8–11].

This is an open-access article distributed under the terms of a Creative Commons Attribution-NonCommercial-ShareAlike 4.0 International Public License, which permits unrestricted use, adaptation, distribution and reproduction in any medium, non-commercially, provided the new creations are licensed under identical terms as the original work and the original work is properly cited.

The crucial event of the capillaries network remodeling under the influence of aging and disease is its rarefaction, leading mechanisms with causal role including left ventricle (LV) pressure overload, endothelial disfunction, reactive oxygen species (ROS), transforming growth factor-beta (TGF-$\beta$)/ROS/Serpinh1 axis or inhibition in vascular endothelial growth factor-A (VEGF-A) mediated angiogenic signaling [8, 12–19].

### Aim

Our current study is the third of a larger project dedicated to the morphological assessment of the myocardial tissue changes primarily related to the ageing process. The current work aimed to compare the variations of myocardial interstitial capillary network density (vascular density – VD) between the main regions of the cardiac wall during the ageing of patients and in relation with different causes of death.

## Patients, Materials and Methods

### Cases

The studied group included 95 patients of different ages and sexes who died from various causes of death and were autopsied in the hospital.

### Studied parameters

#### *Clinical parameters*

The cases were split into subgroups following four clinical criteria and then stratification scales were defined for each subgroup:

▪ *Patients' sex*. Two main scale groups were defined: men (M) and women (F).

▪ *Patients' age*. Four periods of life were defined as follows: childhood and adolescence, 0–24 years, coded as AP_01; young adult, 25–44 years, coded as AP_02; mature adult, 45–64 years, coded as AP_03; and elderly, >64 years, coded as AP_04.

▪ *Cause of death*. Three main categories of causes of death were defined: vascular pathology conditions – V_P; nonvascular pathology conditions – NV_P; and sudden/violent causes of death – S/V_Dth. The latter was also considered as control group (CG).

#### *Morphological parameters*

The only one morphological parameter considered to be assessed was the density of capillaries in the myocardial tissue area, expressed as capillaries/mm$^2$, coded VD.

### Study material

There were two sources of data, namely, deceased patients' medical records for the clinical parameters and myocardial tissue samples collected during autopsies for morphological parameters.

### Tissue sampling

Five epicardium-to-endocardium cross-sections were collected from the third cross-section through the heart, counting from the apex, following a protocol previously designed and updated [20–22]. The cross-sections belonged to the five main topographic regions of the heart wall: **left ventricle wall** (LVW), with three subregions from anterior to posterior [anterior segment (LV_AW), lateral segment (LV_LW), and posterior segment (LV_PW)], **interventricular septum** (IVS) and **right ventricle wall** (RVW) (Figure 1 – center). Tissue samples were selected so that they do not contain visible lesions wall.

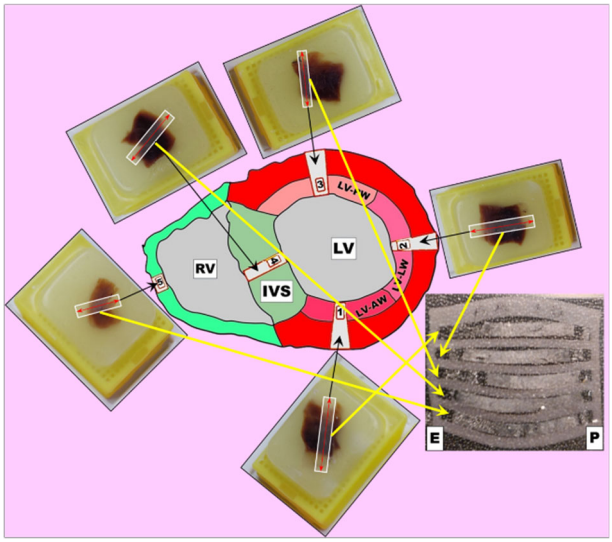


**Figure 1 –** ***The algorithm of sampling. A: Anterior; IVS: Interventricular septum; L: Left; LV: Left ventricle; LV-AW: Anterior left wall; LV-LW: Lateral left wall; LV-PW: Posterior left wall; P: Posterior; R: Right; RV: Right ventricle.***

### Tissue processing

#### *Creating the primary blocks*

Tissue processing followed also a protocol previously designed [22]. Thus, the fragments of myocardial tissue were processed using the classical technique of fixation in 10% solution of buffered formalin at neutral pH followed by paraffin embedding.

#### *Creating the microarray blocks*

From the initial paraffin blocks, 2 mm thick paraffin slices containing myocardial tissue from epicardium to endocardium from each of the five cardiac wall regions described above were cut out and introduced, in order (from 1 to 5) and with epicardial ends on the right, in a modified specially designed biomimetic colloid support matrix (Figure 1 – bottom right) [23–26].

The matrix supports, charged with slices of embedded tissue were reincluded in paraffin, resulting the final tissue microarray (TMA) blocks (Figure 1 – bottom right).

#### *Creating the histological slides*

Further, TMA blocks were cut at 2 mm, obtaining two serial sections: both passed on a regular histological slide and stained with Hematoxylin and Eosin (H&E) and immunomarked with cluster of differentiation 34 (CD34), respectively.

### Quantitative assessment

#### *Slide digitization and image acquisition*

Glass slides were transformed into virtual slides with a Leica Aperio AT2 scanner, using the ×40 objective.

From each of the five topographically heart wall fragments of a case, a region of interest (ROI) was selected from the dedicate Aperio Image Scope program [v12.3.2.8013] (Figure 2, a and b).

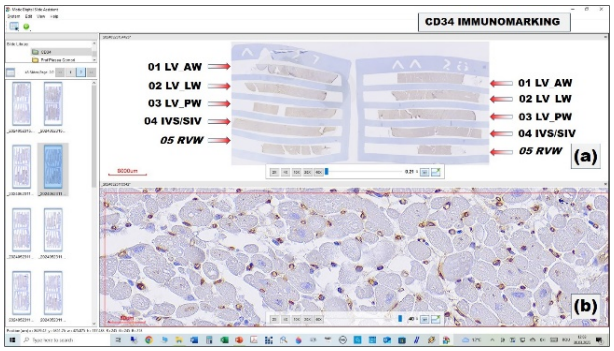


**Figure 2 –** ***Aperio ImageScope virtual slide viewing software window [v12.3.2.8013]: (a) The whole virtual slide; (b) Region of interest (ROI) selection.***

### *Image processing and morphological determinations*

All selected fields from each of the digital slides were exported as red, green, and blue (RGB)–*Joint Photographic Experts Group* (JPEG) images and stored in a single directory and image analysis was performed on the full selected ROI, without additional region selection using the functions incorporated in "Image Processing Toolbox" menu of the MATLAB programming environment (MathWorks, USA).

The algorithm included three steps. The first step of image processing was **staining normalization**. Firstly, a separate image that was considered empirically representative in terms of staining for the whole set of images was selected and used as a staining reference for the normalization process (Figure 3a).

Then, each of the images selected from the digitized slides was normalized with respect to the reference image chosen using a custom color transfer algorithm designed and presented previously [27] that was applied to the LAB color space on each channel in order to reduce the variability in staining/brightness between images.

Next step consisted of the **white background quantification**. Thus, a white-like mask was computed to estimate background/blank tissue area:

1. Images were converted to double precision in [0,1][0,1].
2. The mean intensity across RGB channels was computed per pixel.
3. Channel similarity was enforced by calculating the per-pixel difference between the maximum and minimum channel values.
4. Pixels were classified as white-like if:
   – Mean intensity >> 0.90, and
   – Channel range << 0.06.
5. Small objects were removed with area opening (minimum 100 pixels).
6. A morphological dilation with a disk structuring element (radius 2 px) was applied.
7. Two summary metrics were recorded:
   – Pixel count (total image area) = image height × image width.
   – White pixel count = number of pixels in the white-like mask.

A ***semi-transparent cyan overlay*** (alpha 0.6) was rendered for visual quality control (QC) and saved for each image as seen in Figure 3b.

Next step was the **vessel detection (CD34-positive structures)**. Putative vessels were segmented from the color-normalized RGB images using a simple intensity heuristic targeting brown chromogen signal:

1. The green (G) and blue (B) channels were averaged to form GB=(G+B)/2GB = (G+B)/2 (8-bit).
2. A preliminary "brown" mask was defined by thresholding GB<180.
3. Holes inside detected objects were filled (**imfill with holes**).
4. Morphological opening was performed using a disk structuring element (radius 2 px): erosion followed by dilation.
5. Small objects were removed (**bwareaopen**) with a minimum area of 100 pixels.
6. Connected components were labeled (**bwlabel**), and vessel count was defined as the number of labeled components.

For qualitative review, a ***semi-transparent red overlay*** (alpha 0.6) highlighting the vessel mask was displayed during batch processing (Figure 3c).

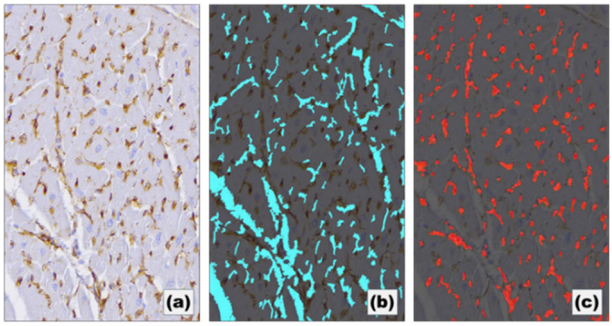


**Figure 3 –** ***Color image processing of CD34 immuno-marked slides: (a) Initial image; (b) Highlighting the "white-like" mask; (c) Highlighting the "red-like" mask. CD34: Cluster of differentiation 34.***

Visual overlays for the white-like mask and the vessel mask were saved as *JPEGs* in dedicated export folders.

The workflow iterated over all image files in the input directory and generated per-image overlays and a summary spreadsheet.

### Quantification and outputs

For each image, the following metrics were recorded:

- Image name.
- Pixel dimension – **PxL**: 0.27 μm.
- Pixel area – **PxA**: PxL × PxL = 0.27 μm × 0.27 μm = 0.0729 μm$^2$.
- Pixel count (total pixels of the image) or image area in pixels – **IAPx** (fixed): 1.273.182/1.303.306 pixels (depending on the resolution of the computer monitor on which the image analysis program used to take the digital photos was installed).
- Vessel count (number of connected components in the post-processed brown mask) – **BOb_CD34**.
- White pixel count (pixels in the white mask – missing tissue/background) – **WPx_CD34**.

Finally, for each image, VD was calculated with the formula:

$$100 \times \frac{BOb_CD34}{IAPx - WPx_CD34}$$

All results were written in an Excel file.

For continuous variables, the following indices were calculated: the lowest value (VMIN), the highest value (VMAX), the average value (AV), standard deviation (STDEV), AV+STDEV, and AV-STDEV. The comparisons were carried out with Pearson's correlation test. Before the statistical comparison between different groups of values, the assessment of the normality of numerical data strings using Lilliefors test. To compare the difference between the average values of VD in the three main regions of the cardiac wall, one-way analysis of variance (ANOVA) – Single Factor test was used.

The graphic illustration and the interpretation of the results were carried out using the "Graph" tool from "Word" and "Excel" modules of the Microsoft Office 2019 Professional software suite and the trial version of XLSTAT 2014 add-on for the "Excel" module.

## Results

### Vascular density

The first step in assessing the density of the capillary vascular network (VD) in the myocardial tissue not affected by lesional processes consisted in determining it for each of the main anatomical segments of the heart wall. Thus, it was observed that the VD on the surface of the uninjured myocardial tissue ($mm^2$) also varied within very wide limits at the level of all three main segments of the heart wall (Figure 4).

The highest variation interval – 3517 capillaries (cp)/$mm^2$ was observed in the RVW, where both the highest maximum value – 4286 cp/$mm^2$ and also the smallest minimum value – 769 cp/$mm^2$ were recorded.

The narrowest range of variation was observed in the LVW – 2736 cp/$mm^2$. Here, the lowest maximum value was also recorded – 3712 cp/$mm^2$. Instead, the highest minimum value was recorded in the IVS – 1252 cp/$mm^2$.

However, the concentration intervals of most values (95%) were much narrower, between two and three times narrower than all values' dispersion ranges, the narrowest being the interval at the LV level – 964 cp/$mm^2$ and the widest being at the RV level – 1346 cp/$mm^2$. They were determined by small values of the STDEVs that varied from 482 cp/$mm^2$ at the LV level to 673 cp/$mm^2$ at the RV level. The intervals were shifted towards the upper limit of the dispersion ranges, more pronounced at the LV and RV levels because they were centered by mean values of the VD that varied between 2686 cp/$mm^2$ at the LV level and 2751 cp/$mm^2$ at the RV level, values clearly higher than half of the dispersion ranges (Figure 4).

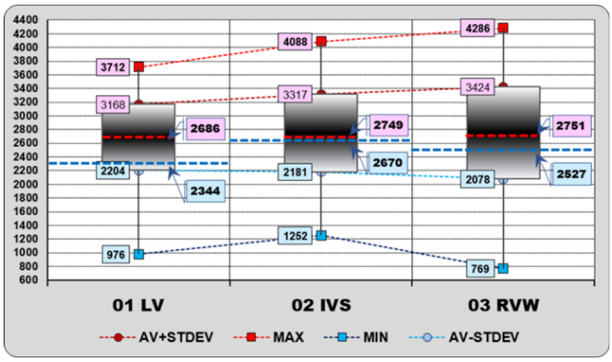


**Figure 4 –** ***Distribution of vascular network density values in each heart segment***

VD increased insignificantly from the LV level to the IVS level and then to the RV level, minimal variation also confirmed by the ANOVA: Single Factor test ($F<F_{crit}$ 0.33<3.02, with a *p*-value of 0.72).

### Variation by age

VD showed a similar pattern of evolution for each of the three main segments of the heart wall with advancing age. Thus, a constant but discrete trend of reduction was observed at the LV and IVS wall level (the Pearson's test *r* coefficient was negative at both segments and discretely lower at the LV level -0.032 *vs* -0.027 and the *p*-values were much higher than the 0.05 reference value (Figure 5).

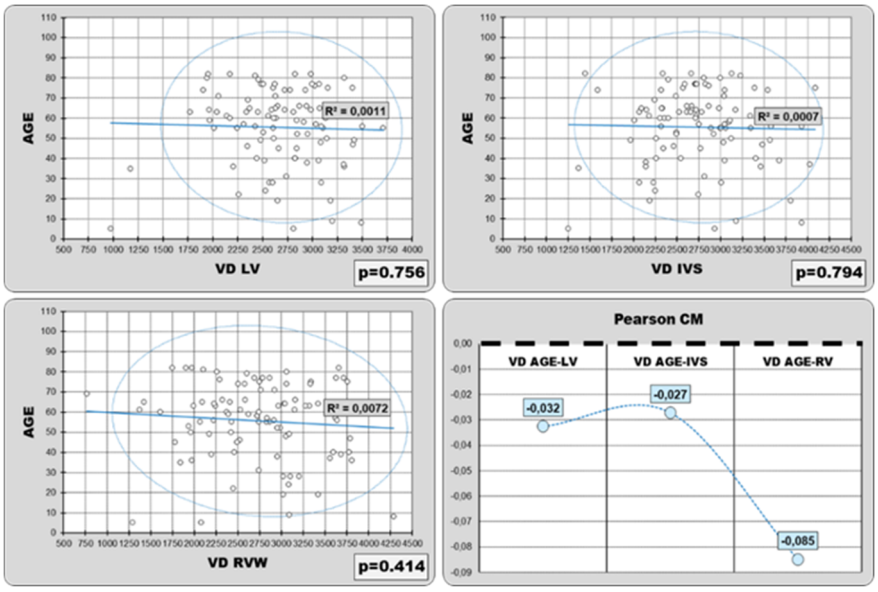


**Figure 5 –** ***Variation in vascular density (VD) values in each of the heart segments according to age.***

In the RV, the reduction in VD with advancing age was more evident, with the negative *r* coefficient of the Pearson's test reducing to -0.085 and the *p*-value being, it is true, higher than the reference value of 0.05 but only 0.414.

When dividing the group of subjects into subgroups according to the period of life, it was observed that the RV undergoes different variations for each of the three main segments of the heart wall from one age period to another (Figure 6). In general, VD values were below the half of values' dispersion range (Figure 6 – black dotted line), except for the values for the RV in the first two periods of life.

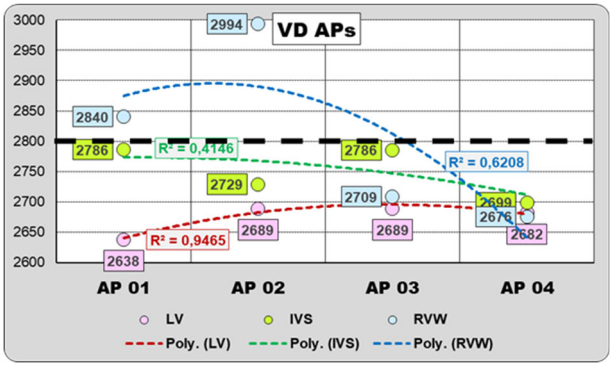


**Figure 6 –** ***Variation of mean vascular density (VD) values for each heart segment according to life periods.***

Then, for the LV, the lowest values of VD were recorded, and the evolution trend was a discrete increasing one towards the mature adult period (AP 03), with a slight decrease towards old age. At the RV level, the increase in VD was significant until the young adult period (AP 02), to then follow a constant evident reduction of VD until old age, where values were recorded significantly lower than those in the first period of life (AP 01).

At the IVS level, the evolution was oscillating, with similar values, high in the AP 01 and AP 03 life periods and the lowest values in old age (AP 04) (Figure 6).

## Variation in the two sexes

The comparison of VD values in the different segments of the heart wall in the two sexes highlighted the fact that, in both men and women, VD had a similar evolution, namely, an obvious and constant increasing trend from the LV level to the RV level, a more attenuated evolution in women towards old age. It is worth noting that VD values were always higher in women than in men (Figure 7).

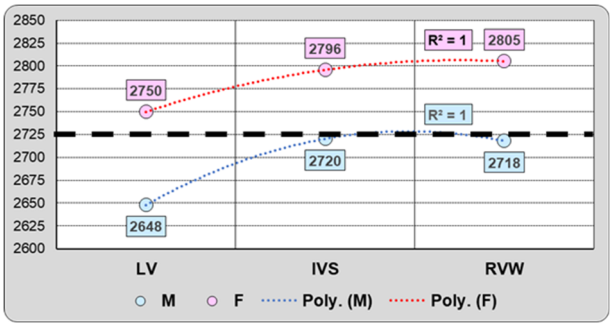


**Figure 7 –** ***Variation of mean vascular density (VD) values for each heart segment in the two sexes.***

It should also be noted that the values recorded in women were above the threshold of half of the dispersion interval of all values (Figure 7 – black dotted line) while the values recorded in men were below this threshold.

### *Evolution with age in both sexes*

Comparative analysis in the two sexes of the way in which the density of intramyocardial capillary vascular structures (VD) evolved at the level of different topographical segments of the heart wall showed that this, like the percentage of muscle fibers (MF), analyzed previously [20], presented in men, with advancing age, a slight increasing trend in all three segments of the heart wall.

The nature of the trend was expressed by the Pearson's test' *p*-value, which was higher than 0.5 reference value (Figure 8 – top). This fact was confirmed by the Pearson's test' *r* coefficient, which was positive (Figure 9 – dotted line with blue values, associated with the blue scale on the left). The trend was accentuated from the LV level to the RV (the Pearson's test *p*-value decreased and the Pearson's test *r* coefficient value increased) (Figure 8 – top; Figure 9 – dotted line with blue values, associated with the blue scale on the left).

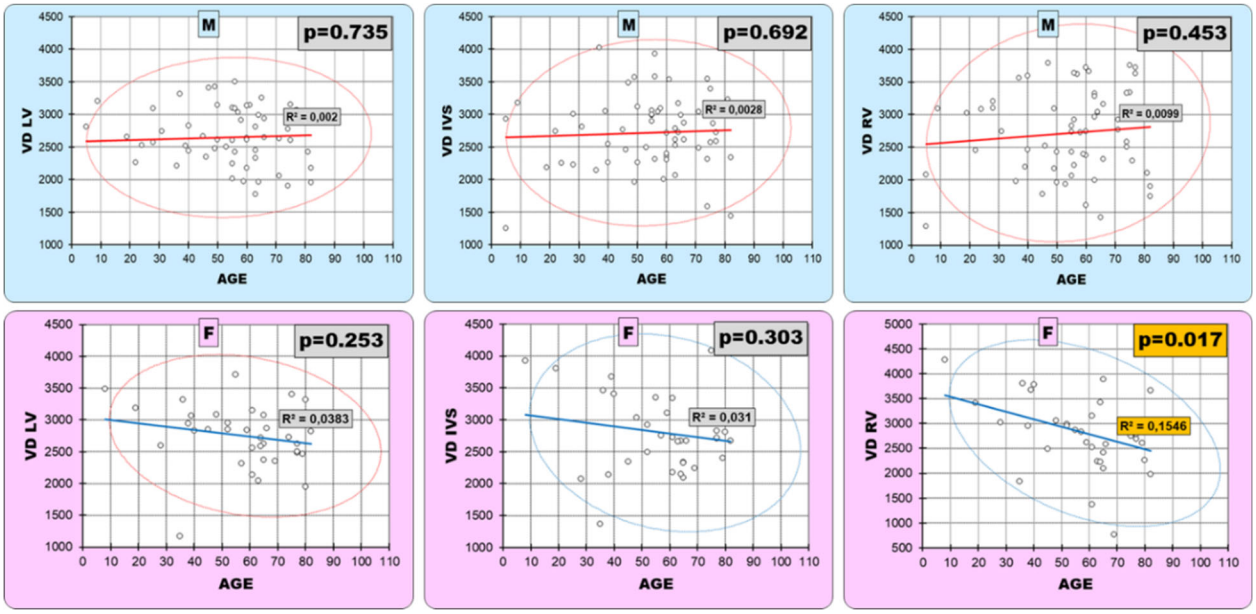


**Figure 8 –** ***Graphical expression of the Pearson's correlation test between the values of the percentage of vascular density (VD) and age. Men: Blue graphs; Women: Pink graphs.***

In women, on the other hand, the trend in the evolution of the VD in all three main segments of the heart wall was decreasing (the *r* coefficient of the Pearson's test was negative; Figure 9 – dotted line with red values, associated with the red scale on the right).

The trend character was expressed by the Pearson's test' *p*-value, which was greater than the 0.5 reference value (Figure 9 – right).

This trend initially decreased between LV and IVS to then become significantly more pronounced at the RV level (the Pearson's test *p*-value increased then decreased significantly and the Pearson's test *r* coefficient value increased slightly then decreased significantly (Figure 8 – bottom; Figure 9 – dotted line with red values, associated with the red scale on the right).

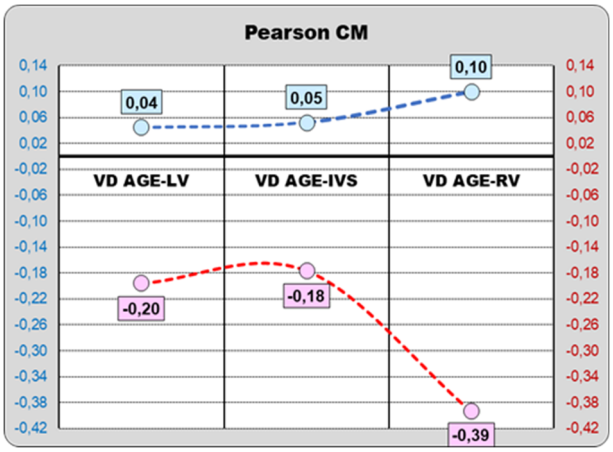


**Figure 9 –** ***Evolution of Pearson's r coefficient values. Men: Blue scale (left); Women: Red scale (right).***

A more detailed analysis, by life periods, of the evolution of VD highlighted different behaviors in the two sexes throughout life.

Thus, in men, the density of capillary vascular structures (VD) had an increasing trend from adolescence to mature adulthood in all three segments of the heart wall, after which there was a decrease towards the third age, likewise, in all three segments of the heart wall but to values higher than those found in adolescence.

The stratification of the values was, in descending order, RV wall, IVS wall and LV wall, in all periods of life (Figure 10 – left). It should also be noted that the values of the VD were always below the half of the values' dispersion range (Figure 10 – left, black dotted line). A more detailed analysis, by life periods, of the evolution of VD highlighted different behaviors in the two sexes throughout life.

Thus, in men, the density of capillary vascular structures (VD) had an increasing trend from adolescence to mature adulthood in all three segments of the heart wall, after which there was a decrease towards the third age, likewise, in all three segments of the heart wall but to values higher than those found in adolescence. The stratification of the values was, in descending order, RV wall, IVS wall and LV wall, in all periods of life (Figure 10 – left). It should also be noted that the values of the VD were always below the half of the values' dispersion range (Figure 10 – left, black dotted line).

In women, on the other hand, VD had a general trend of decreasing throughout life. This trend was a marked and constant one at the RV level with an attenuation towards the third age and a marked one until the young adult period, followed by a slight return in old age at the level of the RV IVS. This marked reduction occurs because in all myocardial wall segments, VD values during adolescence were above the threshold of the half-range of the dispersion of values and fell well below this threshold during the mature adult period (Figure 10 – right, black dotted line).

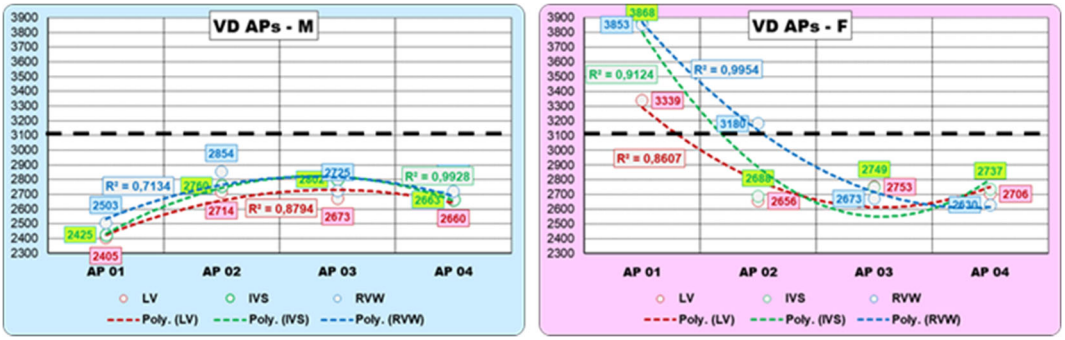


**Figure 10 –** ***Variation of the average values of the vascular density (VD) percentage for each heart segment based on the periods of life in the two sexes.***

## Variation by cause of death

The comparative analysis of the evolution of VD along the three main segments of the heart wall in the different types of pathological conditions that led to the death of the patients revealed different evolutions of it in the three groups. Thus, in the CG and in the V_P group (patients died due to a vascular disease), VD increased constantly from LV to RV, while in the NV_P group (patients died due to nonvascular disease), VD had a general decreasing trend from LV towards RV, but with an increase in the IVS (Figure 11).

All VD values from the V_P group (patients who died due to a vascular disease) were always the lowest compared to those recorded in the other groups and were below the threshold represented by half of the variation interval (Figure 11 – black dotted line).

The highest values were recorded in patients who died from suspicious or violent causes of death (S-V_Dth group). They were clearly located above the threshold represented

by half of the variation interval, as were the VD values recorded in the NV_P group (patients who died from a nonvascular disease) (Figure 11 – black dotted line).

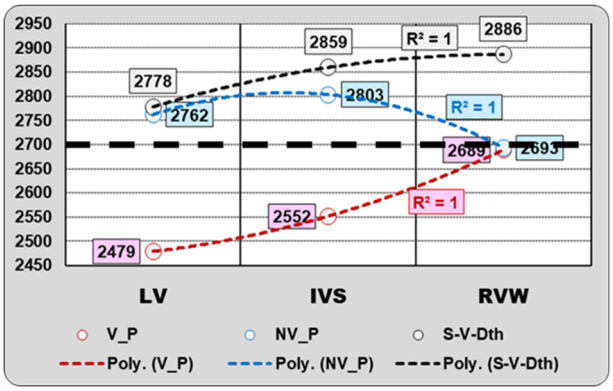


**Figure 11 –** ***Variation in mean vascular density (VD) values at in each heart segment based on the cause of death.***

Comparing how the amount of VD evolved along the main segments of the heart wall in men and women in the three groups of patients with different causes of death showed several differences both from the developments recorded in the entire group and between the two sexes.

The first aspect is the comparison of the stratification of the values recorded in the three groups.

***Evolution by causes of death in both sexes***

Thus, in men the stratification pattern is identical to that observed in the entire groups (Figure 8), only at the IVS level, with the highest values in the S-V_Dth group (CG), followed by the values recorded in the NV_P group (patients who died from a nonvascular disease) and the lowest values in the V_P group (patients who died from avascular disease) (Figure 12 – left).

At the LV level, VD had the highest values in the NV_P group, followed immediately by those in the S-V_Dth group (CG) and, at a significant interval, by those in the V_P group. In contrast, at the RV level, S-V_Dth group (CG) had the highest values, followed immediately by the V_P group. The lowest values occurred in the NV_P group.

In women, the stratification was identical to that observed in the integral groups (Figure 7) but much more clearly defined (S-V_Dth group – CG, NV_P group, and V_P group; Figure 12 – right).

A second aspect would be that of the distribution along the value scale. Thus, in men, the values were, in their vast majority, below the half of the dispersion interval of the values (Figure 12– left, black dotted line). In women, on the other hand, the VD values in the S-V_Dth group (CG) and those in the IVS level of the NV_P group were above the mentioned threshold (Figure 12– right, black dotted line).

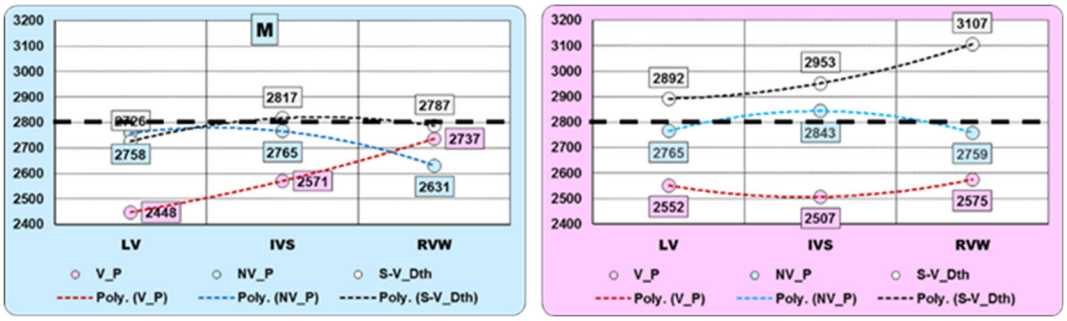


**Figure 12 –** ***Variation in mean values of vascular density (VD) percentage for each heart segment based on the cause of death in the two sexes.***

A third aspect would be the differences between the evolutions and levels of VD in the two sexes for each of the three groups. Thus, in the S-V_Dth group (CG), VD values are higher in women than in men at the in each of the three cardiac walls. Also, the values increase constantly from LV to RV in women, while, in men, they are almost similar in the ventricular walls and slightly higher at the IVS. In the NV_P group, VD values are also higher in women than in men at the for each of the three cardiac walls. In men, the values register a discrete general downward trend from LV to RV. In the V_P group, VD values increased in men constantly towards RV and, from the IVS, except those in women where the values are almost constant (Figure 12).

***Comparative evolution by segments***

The way in which the VD percentages evolved in each of the different segments of the heart wall in relation to each other was, in this case as well, very closely parallel and direct in both men and women, a behavior also confirmed by the statistical apparatus.

Thus, the *p*-values of the Pearson's correlation test between the percentages of VD values in the heart wall segments taken two by two in both men and women were much lower than the 0.05 reference value, namely around 0.0001 (Figure 13). The degree of direct correlation was higher in men when we compared the correlations between the LV and the other two walls, as demonstrated by the values of the Pearson's *r* coefficient. When comparing the IVS–RV correlation, the situation was reversed, the degree of correlation being lower in men than in women.

In men, the degree of correlation decreased from the comparison between anterior segments to the comparison between posterior segments (Figure 14 – blue dotted line, associated with the blue scale on the left).

In women, the values of the Pearson's *r* coefficient test were clearly reduced when we reported LV to RV, and less so when we reported IVS to RV (Figure 14 – red dotted line, associated with the red scale on the right).

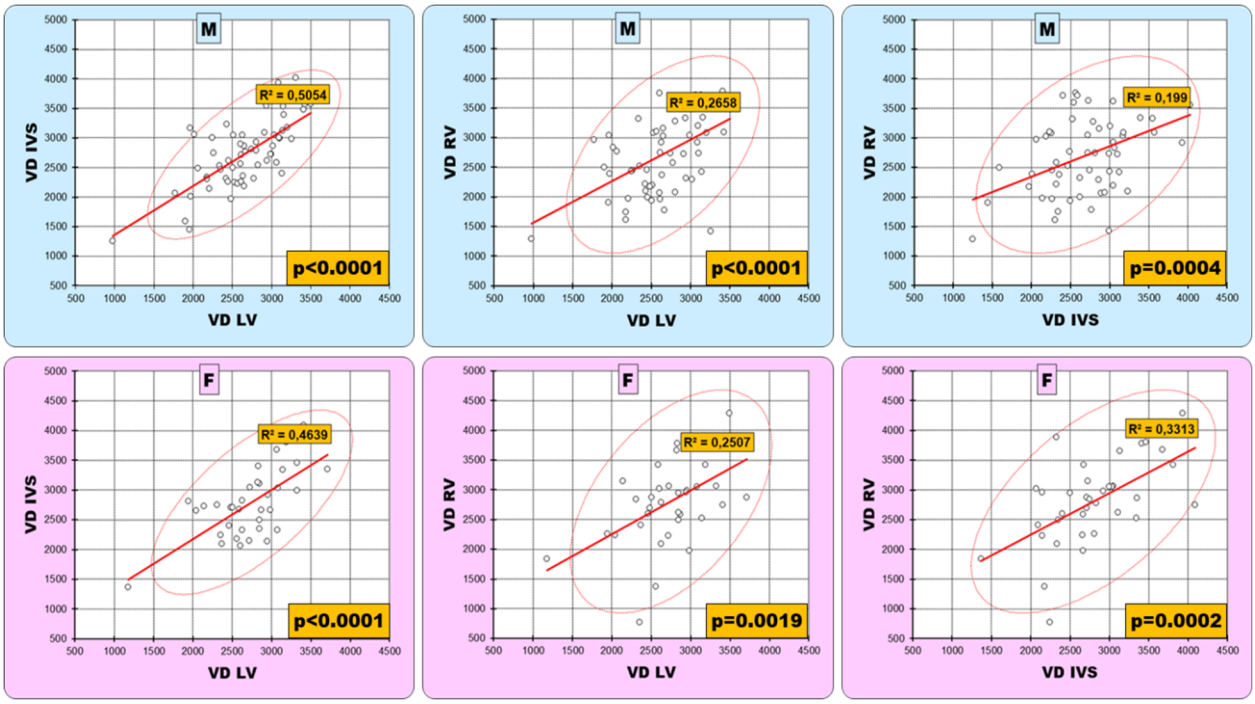


**Figure 13**– ***Graphical expression of the Pearson's correlation test between vascular density (VD) percentages in the cardiac wall segments. Men: Blue graphs; Women: Pink graphs.***

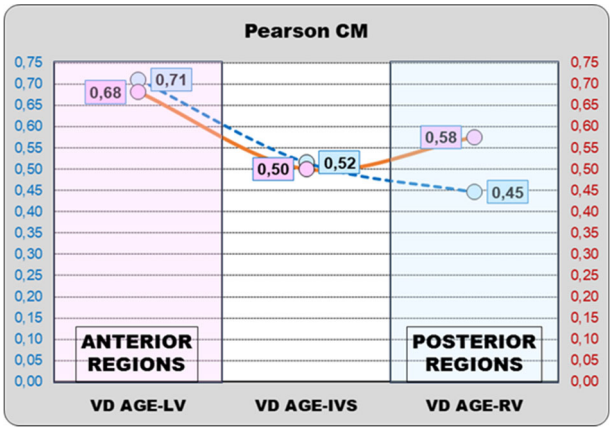


**Figure 14** – ***Evolution of the values of the Pearson's r coefficient test compared between men and women.***

## Discussions

Regarding the behavior of the capillary network in the myocardial interstitium with advancing age, our research showed that the density of the interstitial capillary network increased slowly from youth to senescence in the LVW but decreased with advancing age in the IVS and RVW. It recorded the lowest values in the LVW until the mature adult period and in the RV erectile tissue during senescence. The highest values were recorded in the RV until 44 years of age and then in the IVS.

Comparing the two sexes, it was found that interstitial capillary density showed a higher interstitial capillary density in women than in men along the regions of the heart wall and a divergent behavior in the two sexes with advancing age. Thus, in men, VD increases with age from the LV to the RV while, in women, the trend is decreasing from the LV to the RV with advancing age.

Regarding the behavior of the capillary network in the myocardial interstitium at the level of different segments of the heart wall in people who died from different causes, our research showed that the density of myocardial interstitial capillaries had the lowest values in the V_P group (patients died from a vascular disease) and the highest values in the group of people who died from suspicious/violent causes. Its values increased from the LV to the RV in the V_P group of (patients died from a vascular disease) and the highest values in the group of people who died from suspicious/violent causes and decreased in the NV_P group (patients died from a nonvascular disease).

Comparing the behavior in the two sexes of the capillary network in the myocardial interstitium at the level of different segments of the heart wall in people who died from different causes, the values of myocardial interstitial capillary density were higher in females than in males in the S-V_Dth group (people died from suspicious/violent causes) and in the NV_P group (patients died from a nonvascular disease), and higher in men than in women in the V_P group (patients died from a vascular disease).

Also, its values were lowest in both men and women in the V_P group (patients who died from a vascular disease), but highest in men in the NV_P group (patients died from a nonvascular disease) and in women in the S-V_Dth (group of people died from suspicious/violent causes).

## Conclusions

Regarding the remodeling of heart wall components with advancing age, the vascular compartment, with its two components, myocardial interstitial capillary density and the space occupied by vascular elements, generally had higher values in women than in men, and remodeling

with advancing age had different patterns, both along the regions of the heart wall and in the two sexes.

Regarding the remodeling of wall components in groups of patients who died from different causes of death, the diseases that can cause the death of patients have determined different ways of remodeling the interstitial capillary network both along different segments of the heart wall and in the two sexes, the most important being the decrease in capillary density in the V_P group (patients died from a vascular disease) compared to the other causes of death.

**Conflict of interests**

The authors declare that they have no conflict of interests.

## References


[1] Gu C, Li T, Jiang S, Yang Z, Lv J, Yi W, Yang Y, Fang M. AMP-activated protein kinase sparks the fire of cardioprotection against myocardial ischemia and cardiac ageing. Ageing Res Rev, 2018, 47:168–175. https://doi.org/10.1016/j.arr.2018.08.002 PMID: 30110651

[2] Gupta SK, Foinquinos A, Thum S, Remke J, Zimmer K, Bauters C, de Groote P, Boon RA, de Windt LJ, Preissl S, Hein L, Batkai S, Pinet F, Thum T. Preclinical development of a microRNA-based therapy for elderly patients with myocardial infarction. J Am Coll Cardiol, 2016, 68(14):1557–1571. https://doi.org/10.1016/j.jacc.2016.07.739 PMID: 27687198

[3] Hodes RJ, Sierra F, Austad SN, Epel E, Neigh GN, Erlandson KM, Schafer MJ, LeBrasseur NK, Wiley C, Campisi J, Sehl ME, Scalia R, Eguchi S, Kasinath BS, Halter JB, Cohen HJ, Demark-Wahnefried W, Ahles TA, Barzilai N, Hurria A, Hunt PW. Disease drivers of aging. Ann N Y Acad Sci, 2016, 1386(1):45–68. https://doi.org/10.1111/nyas.13299. PMID: 27943360 PMCID: PMC5373660

[4] Loffredo FS, Steinhauser ML, Jay SM, Gannon J, Pancoast JR, Yalamanchi P, Sinha M, Dall'Osso C, Khong D, Shadrach JL, Miller CM, Singer BS, Stewart A, Psychogios N, Gerszten RE, Hartigan AJ, Kim MJ, Serwold T, Wagers AJ, Lee RT. Growth differentiation factor 11 is a circulating factor that reverses age-related cardiac hypertrophy. Cell, 2013, 153(4):828–839. https://doi.org/10.1016/j.cell.2013.04.015 PMID: 23663781 PMCID: PMC3677132

[5] Biernacka A, Frangogiannis NG. Aging and cardiac fibrosis. Aging Dis, 2011, 2(2):158–173. PMID: 21837283 PMCID: PMC3153299

[6] Grassi G, Seravalle G, Bertinieri G, Turri C, Dell'Oro R, Stella ML, Mancia G. Sympathetic and reflex alterations in systo-diastolic and systolic hypertension of the elderly. J Hypertens, 2000, 18(5):587–593. https://doi.org/10.1097/00004872-200018050-00012 PMID: 10826562

[7] Barry A, Patten B. The structure of the adult heart. In: Gould SE (ed). Pathology of the heart and blood vessels. Charles C. Thomas, Springfield, IL, USA, 1968, 104–105. https://catalog.library.vanderbilt.edu/discovery/fulldisplay/alma991024464659703276/01VAN_INST:vanui

[8] Yoshida Y, Shimizu I, Minamino T. Capillaries as a therapeutic target for heart failure. J Atheroscler Thromb, 2022, 29(7):971–988. https://doi.org/10.5551/jat.RV17064 PMID: 35370224 PMCID: PMC9252615

[9] Berry GJ, Billingham ME. Normal heart. In: Mills SE (ed). Histology for pathologists. 3rd edition, Lippincott Williams & Wilkins, Philadelphia, PA, USA, 2007, 527–544. https://ndl.ethernet.edu.et/handle/123456789/51415

[10] Junqueira LC, Carneiro J. Basic histology: text and atlas. 11th edition, McGraw–Hill Companies, New York, NY, USA, 2005. https://search.worldcat.org/title/Basic-histology-:-text-and-atlas/oclc/761809010

[11] Ferrans VJ, Rodriguez ER. Ultrastructure of the normal heart. In: Silver MD (ed). Cardiovascular pathology. 2nd edition, Churchill Livingstone, New York, NY, USA, 1991, 43–101. https://search.worldcat.org/title/Cardiovascular-pathology/oclc/1483131305

[12] Grunewald M, Kumar S, Sharife H, Volinsky E, Gileles-Hillel A, Licht T, Permyakova A, Hinden L, Azar S, Friedmann Y, Kupetz P, Tzuberi R, Anisimov A, Alitalo K, Horwitz M, Leebhoff S, Khoma OZ, Hlushchuk R, Djonov V, Abramovitch R, Tam J, Keshet E. Counteracting age-related VEGF signaling insufficiency promotes healthy aging and extends life span. Science, 2021, 373(6554):eabc8479. https://doi.org/10.1126/science.abc8479 PMID: 34326210

[13] Nakao M, Shimizu I, Katsuumi G, Yoshida Y, Suda M, Hayashi Y, Ikegami R, Hsiao YT, Okuda S, Soga T, Minamino T. Empagliflozin maintains capillarization and improves cardiac function in a murine model of left ventricular pressure overload. Sci Rep, 2021, 11(1):18384. https://doi.org/10.1038/s41598-021-97787-2 PMID: 34526601 PMCID: PMC8443662

[14] Hemanthakumar KA, Fang S, Anisimov A, Mäyränpää MI, Mervaala E, Kivelä R. Cardiovascular disease risk factors induce mesenchymal features and senescence in mouse cardiac endothelial cells. Elife, 2021, 10:e62678. https://doi.org/10.7554/eLife.62678 PMID: 33661096 PMCID: PMC8043751

[15] Li J, Zeng J, Wu L, Tao L, Liao Z, Chu M, Li L. Loss of *P53* regresses cardiac remodeling induced by pressure overload partially through inhibiting HIF1*α* signaling in mice. Biochem Biophys Res Commun, 2018, 501(2):394–399. https://doi.org/10.1016/j.bbrc.2018.04.225 PMID: 29729274

[16] Obas V, Vasan RS. The aging heart. Clin Sci (Lond), 2018, 132(13):1367–1382. https://doi.org/10.1042/CS20171156 PMID: 29986877

[17] Münzel T, Camici GG, Maack C, Bonetti NR, Fuster V, Kovacic JC. Impact of oxidative stress on the heart and vasculature: Part 2 of a 3-part series. J Am Coll Cardiol, 2017, 70(2):212–229. https://doi.org/10.1016/j.jacc.2017.05.035 PMID: 28683969 PMCID: PMC5663297

[18] López-Otín C, Blasco MA, Partridge L, Serrano M, Kroemer G. The hallmarks of aging. Cell, 2013, 153(6):1194–1217. https://doi.org/10.1016/j.cell.2013.05.039 PMID: 23746838 PMCID: PMC3836174

[19] Rakusan K, Flanagan MF, Geva T, Southern J, Van Praagh R. Morphometry of human coronary capillaries during normal growth and the effect of age in left ventricular pressure-overload hypertrophy. Circulation, 1992, 86(1):38–46. https://doi.org/10.1161/01.cir.86.1.38 PMID: 1535573

[20] Cameniţă LE, Florescu C, Pleşea IE, Şerbănescu MS, Pleşea RM, Lazarovici AR, Martin L. Remodeling of muscular component of the myocardial tissue depending on age, sex and cause of death. Rom J Morphol Embryol, 2026, 67(1):89–96. https://doi.org/10.47162/RJME.67.1.09 PMID: 42402740

[21] Mirea OC, Ancuţa AA, Şerbănescu MS, Postolache P, Uscatu CD, Marin C, Pleşea IE, Chiuţu LC. Analysis of aortic size in subjects died due to cardiovascular and non-cardiovascular events: a necropsy study. Rom J Morphol Embryol, 2014, 55(3 Suppl):1105–1109. PMID: 25607392

[22] Szalay D, Frołow M. Aortic aneurysms. In: Jaeschke R, Gajewski P, O'Byrne PM (eds). McMaster textbook of internal medicine. Medycyna Praktyczna, Kraków, Poland, 2026. https://empendium.com/mcmtextbook/chapter/B31.II.2.22

[23] Gologan D, Ştefan AE, Militaru M, Sanda AC, Arjan S, Muşat S, Leavitt MO, Stan R. Quality assurance and cost reduction in histopathology laboratories using tissue microarrays. Vet Sci, 2023, 10(4):280. https://doi.org/10.3390/vetsci10040280 PMID: 37104435 PMCID: PMC10147037

[24] Ştefan AE, Gologan D, Leavitt MO, Muşat S, Pleşea IE, Stan LGR, Pleşea RM, Militaru M. Tissue microarrays – brief history, techniques and clinical future. Rom J Morphol Embryol, 2020, 61(4):1077–1083. https://doi.org/10.47162/RJME.61.4.10 PMID: 34171057 PMCID: PMC8343478

[25] Musat S. Biomimetic gellable colloid for encoding, processing and sectioning histological samples. International Patent Application No. WO/2016/013949, 2016. https://patentscope.wipo.int/search/en/detail.jsf?docId=WO2016013949

[26] Musat S. Matrix for receiving a tissue sample and use thereof. United States Patent No. US 9851349 B2, 2013. https://patentimages.storage.googleapis.com/f1/ff/26/89c5552d6aa206/US9851349.pdf

[27] Şerbănescu MS, Pleşea IE. A hardware approach for histological and histopathological digital image stain normalization. Rom J Morphol Embryol, 2015, 56(2 Suppl):735–741. PMID: 26429166

***Corresponding authors***

Valentin Titus Grigorean, Professor, MD, PhD, 10th Clinical Department—General Surgery, Faculty of Medicine, Carol Davila University of Medicine and Pharmacy, 8 Eroii Sanitari Avenue, Sector 5, 050474 Bucharest, and Department of General Surgery, Bagdasar–Arseni Emergency Clinical Hospital, 12 Berceni Road, Sector 4, 041915 Bucharest, Romania; Phone +40722–766 144, e-mail: grigorean.valentin@yahoo.com, valentin.grigorean@umfcd.ro

Iancu Emil Pleşea, Professor, MD, PhD, Departments of Pathology, Carol Davila University of Medicine and Pharmacy, and Bagdasar–Arseni Emergency Clinical Hospital, 12 Berceni Road, Sector 4, 041915 Bucharest, Romania; Phone +40722–992 511, e-mail: pie1956@yahoo.com, emil.plesea@umfcd.ro

*Received: June 5, 2026*

*Accepted: July 30, 2026*